Kinetic theory of flocking: Derivation of hydrodynamic equations

Thomas Ihle

Department of Physics, North Dakota State University, Fargo, North Dakota 58108-6050, USA
Max Planck Institute for the Physics of Complex Systems, Nöthnitzer Straße 38, D-01187 Dresden, Germany

It is shown how to explicitly coarse-grain the microscopic dynamics of the rule-based Vicsek model for self-propelled agents. The hydrodynamic equations are derived by means of an Enskog-type kinetic theory. Expressions for all transport coefficients are given. The transition from a disordered to a flocking state, which at large particle speeds appears to be a fluctuation-induced first-order phase transition, is studied numerically and analytically.

Pattern formation and collective motion in systems of self-propelled objects are fascinating phenomena which have attracted much attention. Systems of interest include animal flocks [1], chemically powered nanorods [2], and actin networks driven by molecular motors [3]. Theoretical studies of these systems are usually based on phenomenological transport equations. In most cases, the equations are postulated by means of symmetry arguments, which define only the general form of the terms but leave their coefficients undetermined.

One goal of this Rapid Communication is to provide a systematic derivation of all relevant coefficients for the two-dimensional Vicsek model (VM) of self-propelled particles [4]. In the VM, pointlike particles are driven with constant speed. At each time step, a given particle assumes the average direction of motion of its neighboring particles, with some added noise. As the noise amplitude decreases, the system undergoes a phase transition from a disordered state, in which the particles have no preferred global direction, to an ordered state, in which the particles move collectively in the same direction. This long-range order motivated renormalization group studies by Toner and Tu [5]. They found that the stabilization of the ordered phase is due to the nonzero speed of the particles, allowing two originally distant particles to interact with each other at a later time. The phase transition was originally thought to be continuous [4], but recent numerical work [6] indicates that the transition is discontinuous with strong finite-size effects. There are a few analytical studies on this transition [7,8]; however, they do not treat the original VM but simple models related to it. For example, Bertin *et al.* [7], study a model with simplified interactions and a continuous-time dynamics by means of a Boltzmann equation.

Numerical simulations of the VM [4,6] show localized high-density structures for which a Boltzmann description, which is restricted to low densities, is not sufficient. Enskog's proposal to generalize the Boltzmann equation to dense gases was a major milestone in kinetic theory. In this Rapid Communication, it is shown how an Enskog-type equation with genuine multibody collisions can be obtained for the VM and how this can be used to rigorously derive hydrodynamic equations. In addition to the terms postulated by Toner and Tu [5], the derived equations contain several new relevant terms which describe an intricate coupling between density

and order-parameter gradients. The coefficients of all terms compatible with the symmetries of the system are calculated explicitly in third order of a gradient expansion. The new kinetic equation is used to determine the mean-field phase diagram of the VM, which agrees well with direct numerical simulations but disagrees with the results of a related continuous-time model [7]. This shows the importance of explicitly taking the discrete-time, rule-based nature of the VM into account. The derived hydrodynamic equations are applied to study the stability of a homogeneous flocking state against spatio-temporal perturbations. I discuss how an instability at the onset of collective motion can change the appearance of the phase transition from second to first order. Predictions are given for the system size where this change is expected to happen.

In the VM, a system of N pointlike particles with continuous spatial coordinates $\mathbf{r}_i(t)$ and velocities $\mathbf{v}_i(t)$ evolves via two steps: streaming and collision. During a time step τ, particles stream ballistically: $\mathbf{x}_i(t + \tau) = \mathbf{x}_i(t) + \tau \mathbf{v}_i(t)$. The magnitude of the particle velocities is fixed at v_0. Only the directions θ_i of the velocity vectors are updated in the collision step: a circle of radius R is drawn around a given particle and the average direction $\bar{\theta}_i$ of motion of the particles within the circle is determined according to $\bar{\theta}_i = \arctan[\sum_j^n \sin(\theta_j) / \sum_j^n \cos(\theta_j)]$. The new directions follow as $\theta_i(t + \tau) = \bar{\theta}_i(t) + \xi_i$, where ξ_i is a random number chosen with uniform probability from the interval $[-\eta/2, \eta/2]$. Since explicitly coarse-graining the dynamics of the VM is difficult, in previous work [9] I first validated the formalism on a simpler equilibrium model [10] which shares essential features with the VM. The kinetic formalism starts with the Liouville equation for the N-particle probability density

$$
\begin{aligned}
&P(\theta^{(N)}, \mathbf{X}^{(N)} + \tau \mathbf{V}^{(N)}, t + \tau) \\
&= \frac{1}{\eta^N} \int_{-\eta/2}^{\eta/2} d\xi^{(N)} \int_0^{2\pi} d\tilde{\theta}^{(N)} P(\tilde{\theta}^{(N)}, \mathbf{X}^{(N)}, t) \\
&\quad \times \prod_{i=1}^N \hat{\delta}(\theta_i - \xi_i - \bar{\theta}_i),
\end{aligned} \tag{1}
$$

where $\mathbf{X}^{(N)} \equiv (\mathbf{x}_1, \mathbf{x}_2, \ldots, \mathbf{x}_N)$, $\theta^{(N)} \equiv (\theta_1, \theta_2, \ldots, \theta_N)$, and $\hat{\delta}(x) = \sum_{m=-\infty}^{\infty} \delta(x + 2\pi m)$ is the periodically continued

delta function. The velocities $\mathbf{V}^{(N)} \equiv (\mathbf{v}_1, \mathbf{v}_2, \ldots, \mathbf{v}_N)$, are given in terms of angle variables, $\mathbf{v}_i = v_0(\cos \theta_i, \sin \theta_i)$. The collision integral contains integrations over the precollisional angles $\tilde{\theta}_j$. Assuming that the particles are uncorrelated prior to the collisions, the probability distribution can be expressed as a product of identical one-particle probability distributions: $P(\theta^{(N)}, \mathbf{X}^{(N)}) = \prod_{i=1}^{N} P_1(\theta_i, \mathbf{x}_i)$. This approximation of molecular chaos is valid at moderate and large noise strength η and when the mean-free path (mfp) is large compared to the radius of interaction R. Here, the mfp is defined as the distance a particle travels between collisions, τv_0, and is density-independent due to the discrete nature of the dynamics. Multiplying Eq. (1) by $\sum_i \delta(\mathbf{v} - \mathbf{v}_i) \delta(\mathbf{x} - \mathbf{x}_i)$ and integrating over all particle positions x_i and angles θ_i yields, in the large-N limit [9], a kinetic equation for the one-particle distribution function $f(\theta, \mathbf{x}, t) = N P_1(\theta, \mathbf{x}, t)$,

$$
\begin{aligned}
&f(\theta, \mathbf{x} + \tau \mathbf{v}, t + \tau) \\
&= \frac{1}{\eta} \int_{-\eta/2}^{\eta/2} d\xi \left\langle \left\langle \sum_{n=1}^{N} \frac{e^{-M_R}}{n!} n f(\tilde{\theta}_1, \mathbf{x}, t) \right. \right. \\
&\quad \times \left. \left. \hat{\delta}(\theta - \xi - \bar{\theta}_i) \prod_{i=2}^{n} f(\tilde{\theta}_i, \mathbf{x}_i, t) \right\rangle_{\tilde{\theta}} \right\rangle_x,
\end{aligned} \tag{2}
$$

where $M_R(\mathbf{x}, t) = \int_R \rho(\mathbf{y}, t) \, d\mathbf{y}$ is the average number of particles in a circle of radius R centered around $\mathbf{x}$. The local particle density ρ is given as a moment of the distribution function, $\rho(\mathbf{x}, t) = \int_0^{2\pi} f(\theta, \mathbf{x}, t) d\theta$; $\langle \cdots \rangle_x = \int_R \cdots d\mathbf{x}_2 d\mathbf{x}_3 \cdots \mathbf{x}_n$ denotes the integration over all positions, $n - 1$ particles can assume within the interaction circle; $\langle \cdots \rangle_{\tilde{\theta}} = \int_0^{2\pi} \cdots d\tilde{\theta}_1 d\tilde{\theta}_2 \cdots d\tilde{\theta}_n$ is the average over all pre-collisional angles of n particles in the interaction circle. Since particles in the VM have zero volume, there is a nonzero probability that a large number of particles can be found in the collision circle of a given particle. This leads to the unusual structure of the collision integral in which every term in the sum accounts for an n-particle collision. For example, the $n = 4$ term involves the product of four distribution functions and describes a four-body collision. Interactions between particles which are not at the same position but a distance $\leqslant R$ apart are explicitly taken into account by Eq. (2). This leads to collisional momentum transfer, which is a key feature of the Enskog equation and not included in Boltzmann-type equations. Hence, Eq. (2), can be interpreted as an Enskog-like equation for pointlike particles with discrete time evolution; it remains valid even at infinite density.

Let us first consider a spatially homogeneous system and study stationary solutions of Eq. (2). This amounts to solving the fixed-point equation $f_0(\theta) = C(f_0)$ for the stationary distribution function f_0, where C denotes the right-hand side of Eq. (2). It can be easily checked that the constant distribution $f_0 = \rho_0/(2\pi)$ is a fixed point at any noise and average density, $\rho_0 = N/A$, where A is the area of the system. This solution corresponds to the disordered phase, where all velocity directions occur with equal probability. Below a critical noise $\eta_C(\rho_0)$ there exists another fixed-point solution which breaks rotational symmetry. It has a maximum at some arbitrary angle $\hat{\theta}$ and describes ordered motion into

this direction. The critical noise follows from the condition $\lambda = 1$, with

$$
\lambda = \frac{4}{\eta} \sin\left(\frac{\eta}{2}\right) e^{-M_R} \sum_{n=1}^{N} \frac{n^2 M_R^{n-1}}{n!} I(n).
$$

$$
I(n) = \frac{1}{(2\pi)^n} \int_0^{2\pi} d\theta_1 \cdots \int_0^{2\pi} d\theta_n \cos \bar{\theta} \cos \theta_1. \tag{3}
$$

Here, M_R is equal to $\pi R^2 \rho_0$ and $\bar{\theta}$ is the average angle defined above Eq. (1). The fixed-point equation was solved numerically for $\eta \leqslant \eta_C$. The solution approaches a cosine with vanishing amplitude when η approaches the critical noise. By means of a Fourier cosine series in $\theta - \hat{\theta}$ the behavior at the critical point was extracted analytically. The order parameter, defined as the amplitude g_1 of the first nontrivial Fourier coefficient, is found to behave as $g_1 \propto \sqrt{\eta_C - \eta}$. Thus, the order-disorder transition appears to be continuous with the mean-field critical exponent of $1/2$. Figure 1(a) shows the calculated phase diagram (solid line). Evaluating Eq. (3) in the low-density limit gives $\eta_C \propto R\sqrt{\rho}$. This scaling with the square root of the density agrees with previous numerical [4] and theoretical results [6,7]. However, there is no dependence of the critical noise on the particle speed in the large-mfp limit, which is consistent with numerical simulations of the VM [4,11] but disagrees with the scaling $\eta_C \propto \sqrt{\rho R v_0}$ for $\rho \to 0$ of the continuous model of Ref. [7]. The dashed line in Fig. 1(a) shows that the phase diagram of this model [obtained from Eq. (35) in [7] with $v_0 \tau/R = 5$] does not describe the VM. Evaluating Eq. (3) in the infinite-density limit yields $\eta_C \to 2\pi$. In order to see whether the homogeneous ordered state is stable under time evolution, I derive the hydrodynamic equations by means of a Chapman-Enskog expansion [9,12]. The basic idea behind this expansion is to take the local stationary state as a reference state and expand around it in powers of the hydrodynamic gradients. To systematically account for these gradients, a dimensionless ordering parameter ϵ is introduced, which is set to unity at the end of the calculation. The procedure starts with a Taylor expansion of the left-hand side of Eq. (2) around $(\theta, \mathbf{x}, t)$. The spatial gradients that occur are scaled as $\partial_\alpha \to \epsilon \partial_\alpha$, and multiple time scales t_i are introduced in the temporal gradients. These time scales describe different
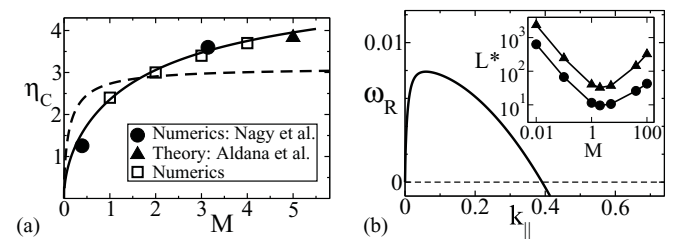

FIG. 1. (a) The critical noise η_C as a function of the average number of collision partners, $M = \rho_0 \pi R^2$, and the prediction of Eq. (35) for large v_0 from Ref. [7], (dashed line) compared with results from Refs. [4,8,11]. (b) Real part of the growth rate ω_R of a small longitudinal perturbation of the ordered state versus dimensionless wave number $k_\parallel$ at $M = 5$, very close to the threshold, $(\eta_C - \eta)/\eta_C = 0.00057$. The inset shows a lower and an upper bound for the crossover length L^* (in units of the mfp), beyond which the phase transition is expected to become discontinuous:

physical processes; for example, in regular fluids, the time scale proportional to ϵ describes convection. For the VM, this is expressed as $\partial_t = \partial_{t_0} + \epsilon \partial_{t_1} + \epsilon^2 \partial_{t_2} + \cdots$.

Expanding the distribution function and the collision integral in powers of ϵ, $f = f_0 + \epsilon f_1 + \epsilon^2 f_2 + \cdots$, and $C = C_0 + \epsilon C_1 + \epsilon^2 C_2 + \cdots$, inserting into Eq. (2), and collecting terms of the same order in ϵ leads to a hierarchy of evolution equations for the f_i. Due to the absence of momentum conservation and Galilean invariance, this set of equations is dramatically different from the usual one. It is not *a priori* evident whether the scaling ansatz for the time derivatives is correct. However, it turns out that this choice avoids any inconsistencies if, additionally, the expansion of the distribution function f is identified as an angular Fourier series with $f_0(\mathbf{x},t) = \rho(\mathbf{x},t)/(2\pi)$ and, for $n > 0$, $f_n(\mathbf{x},\theta,t) = [a_n(\mathbf{x},t)\cos(n\theta) + b_n(\mathbf{x},t)\sin(n\theta)]/(\pi v_0^n)$.

Many moments of the collision integral such as $\langle v_x v_y C_2 \rangle = \int_0^{2\pi} v_x v_y C_2 d\theta$ are required in the Chapman-Enskog expansion. For simplicity, these moments are evaluated in the limit of large mfp: $\tau v_0 \gg R$. This involves solving the following four integrals:

$$J_m(n) = \frac{1}{(2\pi)^n} \int_0^{2\pi} d\theta_1 \cdots \int_0^{2\pi} d\theta_n \Psi_m, \qquad (4)$$

where Ψ_m is given by $\Psi_1 = \cos^2 \bar{\theta} \cos 2\theta_1$, $\Psi_2 = \cos \bar{\theta} \sin \bar{\theta} \cos \theta_1 \sin \theta_2$, $\Psi_3 = \cos \bar{\theta} \cos \theta_1 \cos 2\theta_2$, and $\Psi_4 = \cos \bar{\theta} \cos \theta_1 \cos \theta_2 \cos \theta_3$. The average angle $\bar{\theta}$ is a function of the angles $\theta_1, \theta_2, \ldots, \theta_n$.

We seek a hydrodynamic description of the first two moments of f, namely the particle density $\rho = \int_0^{2\pi} f d\theta$ and the macroscopic momentum density vector $\vec{w} = (w_x, w_y)$, $\vec{w} = \int_0^{2\pi} \vec{v} f d\theta$. Inserting the Fourier representation of f into these moments shows that the first-order coefficients are given by the momentum density, $a_1 = w_x$ and $b_1 = w_y$. Multiplying the hierarchy of evolution equations by powers of the microscopic velocity vector $\vec{v} = (v_x, v_y)$ and integrating over θ gives a set of equations for the time development of the density and the moments a_i and b_i. This analysis is performed in the vicinity of the critical point, $|\lambda - 1| \ll 1$, in order to significantly simplify the consistent closure of the hierarchy of moment equations; see [11].

For simplicity, all equations are rescaled by expressing time in units of τ and distances in units of the mfp, τv_0, which also makes ρ and $\vec{w}$ dimensionless. After straightforward but tedious calculations one obtains the continuity equation $\partial_t \rho + \partial_\alpha w_\alpha = 0$ and a rotationally invariant equation for the momentum density:

$$\partial_t \vec{w} + \nabla \cdot \boldsymbol{H} = -b \nabla \rho + (\lambda - 1)\vec{w} + \boldsymbol{Q_1} \cdot \vec{w} + \boldsymbol{Q_2} \cdot \nabla \rho, \tag{5}$$

with $b = (3 - \lambda)/4$. The momentum flux tensor $\boldsymbol{H}$ and the tensors $\boldsymbol{Q_1}$, $\boldsymbol{Q_2}$

$$\boldsymbol{H} = \sum_{i=1}^{5} h_i \boldsymbol{\Omega_i}, \quad \boldsymbol{Q_1} = \sum_{i=1}^{5} q_i \boldsymbol{\Omega_i}, \quad \boldsymbol{Q_2} = \sum_{i=1}^{5} k_i \boldsymbol{\Omega_i}, \tag{6}$$

are given in terms of five symmetric traceless tensors $\boldsymbol{\Omega_i}$:

$$\Omega_{1,\alpha\beta} = \partial_\alpha w_\beta + \partial_\beta w_\alpha - \delta_{\alpha\beta} \partial_\gamma w_\gamma,$$
$$\Omega_{2,\alpha\beta} = 2\partial_\alpha \partial_\beta \rho - \delta_{\alpha\beta} \partial_\gamma^2 \rho,$$

TABLE I. Transport coefficients h_j, q_j, and k_j, defined in Eq. (6), expressed as functions of Γ, S, p, q; see Eq. (8).

j	h_j	q_j	k_j
1	$\dfrac{1+p}{8(p-1)}$	$\dfrac{S}{2(p-1)}$	$\dfrac{S}{8(p-1)}$
2	$-\dfrac{p^2+10p+1}{96(p-1)^2}$	$-\dfrac{S}{4(p-1)^2}$	$-\dfrac{S(p+5)}{96(p-1)^2}$
3	$-\dfrac{q}{2(p-1)}$	$\Gamma - \dfrac{Sq}{p-1}$	$\dfrac{\Gamma}{4} - \dfrac{Sq}{4(p-1)}$
4	$\dfrac{q(1+p)}{4(p-1)^2}$	$\dfrac{\Gamma}{2} - \dfrac{Sq(p-3)}{2(p-1)^2}$	$\dfrac{\Gamma}{12} - \dfrac{Sq(p-4)}{12(p-1)^2}$
5	$-\dfrac{q(p^2+10p+1)}{48(p-1)^3}$	$\dfrac{\Gamma}{24} - \dfrac{Sq(p^2-2p+13)}{24(p-1)^3}$	$-\dfrac{Sq(p+5)}{48(p-1)^3}$

$$\Omega_{3,\alpha\beta} = 2w_\alpha w_\beta - \delta_{\alpha\beta} w^2, \tag{7}$$
$$\Omega_{4,\alpha\beta} = w_\alpha \partial_\beta \rho + w_\beta \partial_\alpha \rho - \delta_{\alpha\beta} w_\gamma \partial_\gamma \rho,$$
$$\Omega_{5,\alpha\beta} = 2(\partial_\alpha \rho)(\partial_\beta \rho) - \delta_{\alpha\beta}(\partial_\gamma \rho)^2.$$

The tensor Ω_1 is the viscous stress tensor of a two-dimensional fluid. The transport coefficients in Eq. (6) are given in Table I. They depend on the following variables:

$$p = \frac{4}{\eta} \sin(\eta) \sum_{n=1}^{N} \frac{e^{-M_R}}{n!} n^2 M_R^{n-1} J_1(n),$$

$$q = \frac{4\pi\gamma^2}{\eta} \sin(\eta) \sum_{n=2}^{N} \frac{e^{-M_R}}{n!} n^2 (n-1) M_R^{n-2} J_2(n),$$

$$S = \frac{8\pi\gamma^2}{\eta} \sin\frac{\eta}{2} \sum_{n=2}^{N} \frac{e^{-M_R}}{n!} n^2 (n-1) M_R^{n-2} J_3(n), \tag{8}$$

$$\Gamma = \frac{8\pi^2\gamma^4}{3\eta} \sin\frac{\eta}{2} \sum_{n=3}^{N} \frac{e^{-M_R}}{n!} n^2 (n-1)(n-2) M_R^{n-3} J_4(n),$$

where γ is the ratio of the interaction radius to the mfp, $\gamma = R/(\tau v_0)$. Equation (5) is consistent with the one postulated in Ref. [5] but contains additional gradient terms. It has a homogeneous flocking solution: $\vec{w} = w_0 \hat{\mathbf{n}}$ and $\rho = \rho_0$. The amplitude of the flow is given by $w_0 = \sqrt{(1-\lambda)/q_3}$. In order to study the spontaneous onset of collective motion, a perturbation around this state is considered, $\rho(\mathbf{x},t) = \rho_0 + \delta\rho e^{i\mathbf{k}\cdot\mathbf{x}+\omega t}$, $\vec{w}(\mathbf{x},t) = w_0 \hat{\mathbf{n}} + \delta\vec{w} e^{i\mathbf{k}\cdot\mathbf{x}+\omega t}$, and Eq. (5) is linearized in $\delta\rho$ and $\delta\vec{w}$. The characteristic equation for the growth rate $\omega(\vec{k})$ describes three possible modes. I found that, in a small window, $\eta_S < \eta < \eta_C$, directly below the onset of flocking, one of the longitudinal modes is always unstable against long-wavelength perturbations: the real part of ω is positive for $0 < k < k_0$ as shown in Fig. 1(b). A similar instability was reported in Refs. [7,13]. Chaté *et al.* [6] found numerically that the order-disorder transition is discontinuous for system sizes L larger than the crossover length L^*. Assuming that the long-wave instability is the reason for this finite-size effect, I calculated the largest value of k_0 within the narrow instability window at constant density k^* in order to obtain a lower bound for L^*. Plotting $2\pi/k^*$ gives the lower curve in the insert of Fig. 1(b). An upper bound was obtained by determining the

wave number k_{max} where the growth rate has the largest value inside the instability window. The upper curve in the insert shows $2\pi/k_{max}$ as a function of density. The minimum around $M \approx 2$ and the divergences at small and large densities are consistent with numerical results [6].

To see what happens to a growing perturbation beyond the linear instability, the continuity equation and Eq. (5) were integrated on an $L \times L$ lattice with periodic boundaries by means of a predictor-corrector scheme [14]. These simulations confirmed that the ordered phase is stable for small system sizes $L < 2\pi/k_0$. For slightly larger system sizes one observes a stable, inhomogeneous steady state with a global order parameter, $\langle \vec{w} \rangle = \int \vec{w} \, d\mathbf{x}/L^2$, larger than the amplitude of the homogeneous state, w_0. Finally, for much larger system sizes, it turns out that the system is both linearly and nonlinearly unstable for $\eta_S < \eta < \eta_C$. Longitudinal perturbations grow without bound; they do not lead to stable solitons as suggested in Ref. [7]. However, direct simulations of the VM at large mfp do show solitary structures such as traveling high-density bands in a window just below the transition [6,11]. At lower noise these structures disappear. Identifying this "solitary" window with the instability window, its size can be predicted by the current theory which takes all the details of the VM such as multibody interactions into account. However, inside this window, the hydrodynamic equations are driven out of the range of their validity and are not suited to describe solitons. Nagy *et al.* [4] did not see high-density bands at smaller velocities v_0. To treat this limit of small mfp theoretically, one has to abandon the molecular chaos approximation; that is, go beyond the mean-field approximation, which is outside the scope of this paper.

In summary, a first-principle derivation of the hydrodynamic equations of the VM by means of a kinetic theory is presented and a stability analysis of the resulting equations, Eq. (5), is performed. The mean-field phase diagram for arbitrary density is calculated. It agrees to within a few percent with simulation results and is shown to be independent of the particle speed in the large-mfp limit. It is also shown that the continuous theory of Ref. [7] fails to reproduce the phase diagram of the VM and that one has to explicitly incorporate the discrete-time dynamics and genuine multibody interactions in order to achieve agreement. The theory presented here is consistent with numerical studies [4,6] and suggests the following picture of the nature of the flocking transition in the large-mfp limit considered here: At $\eta = \eta_C$ a homogeneous ordered state bifurcates continuously from the disordered state. At the threshold, this state is unstable to longitudinal, long-wavelength fluctuations. Perturbations from a large range of wave numbers $k < k_0$ become unstable, already in close vicinity to the threshold. The transition appears to be continuous in small systems but becomes a discontinuous transition in large systems due to the emergence of density waves which abruptly increase the global order parameter. An estimate is given of the system size L^*, above which the fluctuation-driven discontinuous nature of the transition is expected to emerge. This length is found to diverge at small and large densities, which is consistent with numerical results.

[1] I. D. Couzin *et al.*, Nature (London) **433**, 513 (2005).

[2] Y. G. Tao and R. Kapral, Soft Matter **6**, 756 (2010).

[3] J. F. Joanny *et al.*, New J. Phys. **9**, 422 (2007).

[4] T. Vicsek, A. Czirok, E. Ben-Jacob, I. Cohen, and O. Shochet, Phys. Rev. Lett. **75**, 1226 (1995); A. Czirók, H. E. Stanley, and T. Vicsek, J. Phys. A **30**, 1375 (1997); M. Nagy, I. Daruka, and T. Vicsek, Physica A **373**, 445 (2007).

[5] J. Toner and Y. Tu, Phys. Rev. E **58**, 4828 (1998).

[6] G. Grégoire and H. Chaté, Phys. Rev. Lett. **92**, 025702 (2004); H. Chaté, F. Ginelli, G. Gregoire, and F. Raynaud, Phys. Rev. E **77**, 046113 (2008); H. Chaté, F. Ginelli, and G. Gregoire, Phys. Rev. Lett. **99**, 229601 (2007).

[7] E. Bertin, M. Droz, and G. Grégoire, Phys. Rev. E **74**, 022101 (2006); J. Phys. A **42**, 445001 (2009).

[8] M. Aldana, V. Dossetti, C. Huepe, V. M. Kenkre, and H. Larralde, Phys. Rev. Lett. **98**, 095702 (2007).

[9] T. Ihle, Phys. Chem. Chem. Phys. **11**, 9667 (2009).

[10] G. Gompper, T. Ihle, D. M. Kroll, and R. G. Winkler, Adv. Polym. Sci. **221**, 1 (2009).

[11] T. Ihle and A. Gebremariam (unpublished).

[12] D. A. McQuarrie, *Statistical Mechanics* (Harper & Row, New York, 1976).

[13] S. Mishra, A. Baskaran, and M. C. Marchetti, Phys. Rev. E **81**, 061916 (2010).

[14] R. W. MacCormack, AIAA J. **20**, 1275 (1982).